

Observation of dark spatial photovoltaic solitons in planar waveguides in lithium niobate

V Shandarov[†], D Kip[‡], M Wesner[‡] and J Hukriede[‡]

[†] State University of Control Systems and Radioelectronics, 40 Lenin Ave, Tomsk 634050, Russia

[‡] Fachbereich Physik, Universität Osnabrück, 49069 Osnabrück, Germany

Received 31 March 2000, in final form 27 June 2000

Abstract. We have obtained photovoltaic lenses and dark spatial solitons in planar optical waveguides in lithium niobate doped with iron and copper. For TE modes of lower indices the photovoltaic nonlinearity only partly decreased the width of a dark notch within the outcoupled image of the recording light beam. The corresponding time to reach a steady state of this light-induced change ranged from about 0.1 to 30 s depending on the waveguide sample. For higher modes we observed a full compensation of the divergence of the dark notch on a time scale of some minutes. In some cases this was followed by an extinction of the dark solitons because the light was over-defocused in the highest modes.

Keywords: Spatial soliton, photovoltaic effect, waveguides, LiNbO₃

1. Introduction

Since 1992, when it was shown that photorefractive crystals can give rise to self-guided optical light waves [1], many investigations have been devoted to these so-called photorefractive solitons. This increased interest is caused by the unique properties of solitons in nonlinear propagation and their interaction with each other [2], which makes spatial solitons promising candidates for new developments in all-optical information technology. Bright solitons are light beams that do not change their transverse profile during propagation. To overcome the natural diffraction, a focusing nonlinearity that balances the divergence of the beam is necessary. Dark solitons [3], by the same definition, are dark stripes or notches in an otherwise homogeneous intensity background, which do not change their profile during propagation, either. In this case, a self-defocusing nonlinearity acting upon the illuminated parts balances the diffraction of the dark notch.

Spatial solitons that occur in photorefractive crystals are induced by two different charge transport mechanisms: first, the photovoltaic effect that produces an internal electric field, and second, the drift mechanism in an externally applied electric field. Both mechanisms can result in a refractive index change via the electro-optic effect, which causes focusing/defocusing of a bright/dark single beam, respectively. In LiNbO₃ the photovoltaic effect leads to self-defocusing [4]. Therefore, only the excitation of dark photovoltaic spatial solitons is possible under common conditions [5].

In a one-dimensional model, the refractive index change for charge transport due to the photovoltaic effect may be expressed in the form [3]

$$\Delta n_s \sim AI(z)[I_d + I(z)]^{-1},$$

where A is a constant, $I(z)$ is the intensity profile and z is the transverse direction, and I_d is the dark irradiance. From the experimental point of view, to form a photovoltaic soliton there are only limited possibilities to vary the strength of the nonlinearity that is responsible for soliton formation. Practically, only the involved intensities, $I(z)$ and I_d , can be changed, whereas for the drift-field-induced soliton the size of the nonlinearity can easily be modified by variation of the external electric field.

So far, photovoltaic solitons have been studied solely in three-dimensional (bulk) media [4, 5]. No investigations have been carried out using a two-dimensional or waveguide sample. In a graded-index planar photorefractive waveguide the size of the nonlinearity can vary with depth [6], thus for different modes propagating in different effective depths different soliton solutions can be found, often with significantly different time constants. Such graded-index waveguides in LiNbO₃ can be easily formed, e.g. by indiffusion of different amounts of photorefractive impurities, such as Fe or Cu. The main aim of this work is the realization of dark spatial photovoltaic solitons in different LiNbO₃ planar waveguides fabricated by indiffusion of titanium, iron and copper and the study of their features.

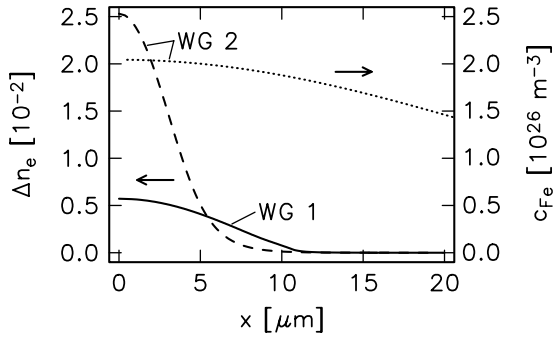


Figure 1. Refractive index profiles for extraordinary polarization for WG1 and WG2 and Fe concentration in WG2.

2. Optical waveguide formation

Planar waveguides have been formed in *y*-cut LiNbO₃ wafers (optical grade, congruently melting composition) by diffusion of Fe only (sample WG1), Ti and Fe (WG2), and Ti, Fe and Cu (WG3). The sample WG1 was formed by indiffusion of a 40 nm thick evaporated Fe layer for 8 h at 1000 °C in air. For the WG2 and WG3 samples first a 74 nm thick Fe layer was indiffused into the wafers at 1000 °C for 20 h in air. Then they were doped with Ti from 100 nm thick films, indiffused at 1000 °C for 24 h in air. Finally, the sample WG2 was annealed in a reducing argon atmosphere for 2 h at 1000 °C. The sample WG3 was additionally Cu doped by indiffusing a 26 nm thick evaporated layer for 2 h at 1000 °C in a reducing argon atmosphere.

For the sample WG1 the indiffused Fe is responsible for both the formation of the Gaussian-like refractive index profile and the photorefractive doping, resulting in different effective Fe concentrations C_{Fe} inside the sample for different modes of the waveguide. On the other hand, in the samples WG2 and WG3 the Ti presence is mainly responsible for the refractive index profile. In the region where light is guided, the concentration C_{Fe} changes only slightly, and the contribution of Fe (and Cu as well) to the refractive index change is negligible. The Fe concentration and refractive index profiles of the samples WG1 and WG2 are illustrated in figure 1.

3. Experimental set-up

The experimental set-up is shown schematically in figure 2. The recording and the probe beams are formed by two helium–neon lasers (wavelength 632.8 nm) and were coupled into the waveguide using either prism or endface coupling. The light was polarized along the *c*-axis (*z*-direction) and the propagation was along *x*. The *y*-direction coincides with the waveguide normal. The beam expander (BE), cylindrical lens (CL) and spherical lens (SL) enabled the adjustment of the necessary dimensions of the recording beam used for the prism coupling. For endface coupling a 20× microscope lens was used instead of a SL. The probe beam was launched into the light path of the recording beam via the mirror M and the beam splitter (BS). The light propagation distance was 5 mm in the experiments with prism coupling and 20 mm for endface coupling.

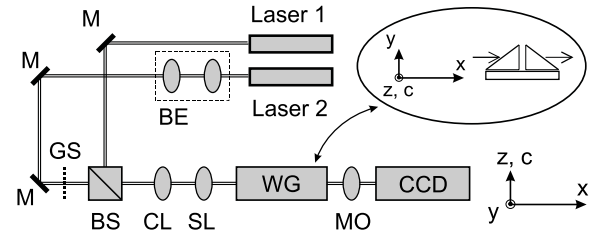


Figure 2. Experimental setup. Laser 1, laser 2—He–Ne lasers; BE—beam expander; M—mirrors; BS—beam splitter; CL—cylindrical lens; SL—spherical lens; MO—microscope objectives; GS—glass slide; CCD—CCD camera.

For dark soliton formation a dark notch in the centre of the recording beam is necessary. This was generated by a thin glass slide that covered one half of the beam, producing a phase shift of $(2m + 1)\pi$, where *m* is an integer. Tilting the glass plate allowed for the adjustment of the correct phase shift. The recording beam power P_{in} ranged from 0.3 to 20 mW, whereas the power of the probe beam was 0.12 mW. The polarization of both beams corresponded to extraordinary waves (TE modes of the waveguide), taking advantage of the large values of both the electro-optic and photovoltaic coefficients of LiNbO₃ for such a polarization and propagation direction. The light that was propagating in the waveguide was coupled out using either a second coupling prism or via the polished endface, and then imaged onto the CCD camera.

It should be noted that in these experiments we did not use any background illumination, as was the case in other experiments with photovoltaic solitons [4, 7]. Due to the high Fe concentrations in our waveguides the dark conductivity was rather high and additional illumination was not necessary.

4. Experimental results and discussion

Self-focusing and dark soliton formation was studied in two different schemes for coupling light into the waveguide: prism coupling (excitation of discrete modes) and endface coupling (excitation of all modes of the sample simultaneously). In both cases the induced refractive index changes can be monitored using a second probe beam that reads out the light-induced waveguide channel.

4.1. Prism coupling

At first, we used the prism-coupling setup. The input beam was focused onto the entrance face of the first coupling prism. Then the development of the dark notch in the light pattern that is outcoupled from the waveguide by a second prism was monitored with help of a CCD camera. The time evolution of the images allowed for an estimation of the dielectric relaxation times corresponding to the different TE modes in our three waveguides. After switching on the recording light we observed a decrease of the width of the dark notch at the position of the outcoupling prism in all three samples. An example is shown in figure 3(a). The final width of the notch in the steady state depends on the input light intensity. The

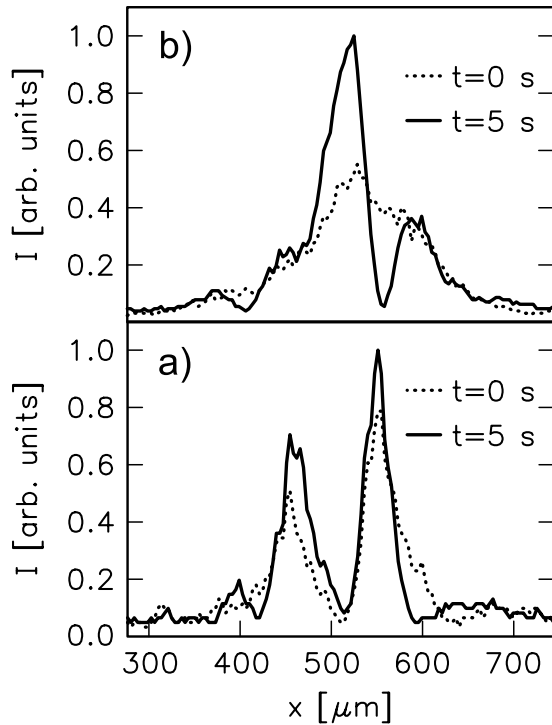


Figure 3. Intensity distribution of the recording beam (a) and the probe beam (b), before ($t = 0$ s) and after ($t = 5$ s) refractive index channel formation in the prism coupling configuration.

characteristic time constants for a typical input power of 1–2 mW were similar for the different TE modes in WG2 (about 0.08–0.1 s) and WG3 (about 10–12 s), and changed from about 5 to 30 s for the sample WG1. This different behaviour is the result of an almost constant iron concentration C_{Fe} for all modes of the titanium-diffused waveguiding layers of samples WG2 and WG3, whereas C_{Fe} significantly changed for different modes of sample WG1.

The probe beam was used to detect the waveguiding channel (or the light-induced photovoltaic lens), which is formed by the dark notch because of the extraordinary refractive index decrease in the illuminated region. As an example, in figure 3(b) we show the intensity distribution of this probe beam in a region where the dark photovoltaic soliton (or the lens mentioned above) for the TE₁ mode of sample WG1 has been formed. Here the steady state of the written channel was obtained after about 5 s; we did not observe any changes in the outcoupled pattern of the recording beam after this time. Because the probe beam was broader than the dark notch (about 50 μm at the position of the incoupling prism), only part of its intensity was trapped inside the channel. After the recording beam was switched off, the probe beam recovered to its original intensity profile within 30–50 s. This allows for an estimation of the erasure time of the formed channel by the intensity of the probe beam. Similar results were observed for the other modes of the same waveguide and for the two other samples.

From the experiment described above we cannot distinguish whether we already have a soliton or just a focusing nonlinearity (a ‘focusing’ of the dark notch due to the light-induced lens). In our experiment the width of the dark notch at the input face of the incoupling prism was

about 25 μm . At the position of the outcoupling prism it was about 80 μm in the linear regime (for low intensity) and about 65 μm in the nonlinear regime. This change of the width may correspond to a dark soliton that is formed after a short propagation distance of the beam in the waveguide. From the corresponding existence curve we estimated for this configuration (corresponding crystal parameters and a ratio of beam intensity to dark irradiance of about 10^{-2} for the lowest modes [8]) a soliton width of about 60 μm [3], which is in reasonable agreement with the value given above. A more exact proof of the soliton regime would require a modified experimental configuration suitable for a direct inspection of the light track within the waveguides over the whole propagation length, which was not possible here.

4.2. Endface coupling

Then we used the endface-coupling method, which results in a simultaneous excitation of all guided TE modes of the waveguide. Because in sample WG1 different modes showed significant differences in their photorefractive parameters that are due to different Fe concentrations, some special features can be expected in exciting all modes at the same time. For the samples WG2 and WG3 with only small changes of the Fe concentration within the waveguiding layer we expected only small differences in the endface coupling scheme. However, even in these waveguides we observed some differences of the photovoltaic lens development compared with that in prism coupling.

Up to recording times necessary to reach the steady state in the prism-coupling scheme, i.e. about 20 s for a recording beam power of 1 mW, a self-focusing of the dark notch similar to the prism-coupling scheme could be observed. However, for longer recording time a further, more significant decrease in the width of the dark notch started. A steady state was not reached up to times of some minutes, sometimes followed by a complete extinction of the notch. Only for light powers lower than 0.5 mW was the dark notch still observed in the steady state. Above this value, the time necessary for complete extinction was strongly dependent on the recording light intensity. It changed from 27 min for a light power of 1 mW to 50 s for a light power of 11.5 mW.

In figure 4, the recording beam was switched off before the light-induced waveguide disappeared. Then the probe beam was used to test the remaining channel. The recording time was 40 s and $P_{\text{in}} = 2$ mW. In this figure the intensity distribution in the direction of the waveguide normal (y -direction, see figure 2) has been measured. We observed a change of the light intensity distribution near the waveguide surface on a time scale of some seconds: the centre of gravity of the outcoupled intensity moves in the direction of the substrate with time. After erasure of that part of the channel which is mainly formed by the intensity guided in the lower modes (close to the surface), we observed a remaining, buried waveguide channel resulting only from the intensity guided in the highest modes of the waveguide. Similar buried waveguide channels could be stored in the dark for times up to some hours without noticeable changes. In figure 5 we illustrate this result for longer recording times. Here the intensity distributions of the recording and probe beam before

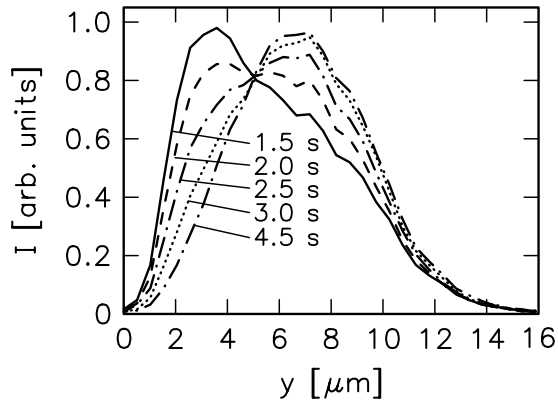


Figure 4. Intensity distribution of the probe beam profile, perpendicular to the waveguiding layer. At $t = 0$ s the recording beam is switched off.

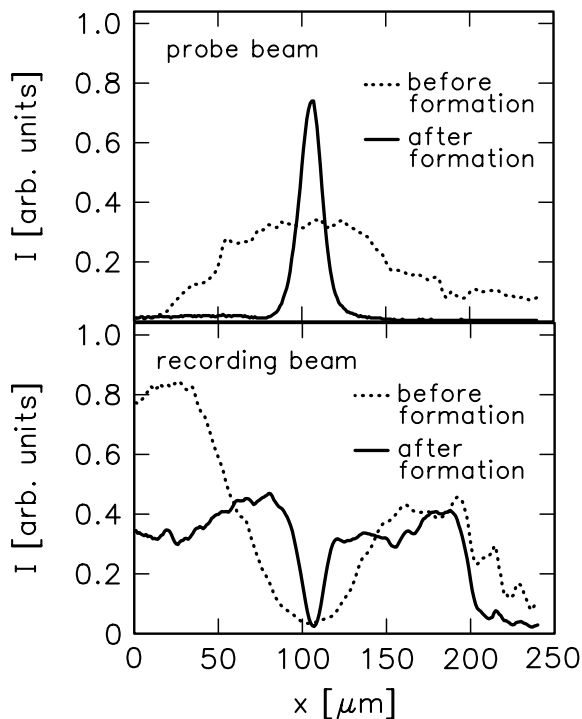


Figure 5. Intensity distribution of the recording beam (lower picture) and the probe beam (upper picture), before and after soliton formation, in the endface-coupling configuration.

and after the formation of the nonlinear lens (or soliton) are presented.

These experimental observations may be explained by excitation of TE modes that are not amenable to prism coupling, i.e. the highest modes with effective refractive indices close to the substrate value of LiNbO₃. These modes are a direct consequence of the more deeply indiffused Fe layer (compared with Ti that is concentrated closer to the surface, see figure 1) that slightly increases the refractive index deep in the waveguide where almost no Ti is present. It is well known, that the excitation efficiency of guided modes in the prism-coupling scheme sharply decreases with the increase of their effective depth, whereas for the endface-

coupling scheme light can be effectively coupled into these deep TE modes. Thus, when we excite a variety of TE modes in the waveguide, some of them may form dark photovoltaic solitons and some others may just form photovoltaic lenses. At the same time for some of the highest modes the optical nonlinearity may be already too high, leading to ‘over-defocusing’ of their light fields. In the case of dominating dark conductivity, the time constant τ for soliton formation of a certain mode is determined by the average dark conductivity σ_d , which is known to decrease with waveguide depth, i.e. for higher modes. Thus, the ‘over-defocusing’ of light for the highest modes starts when spatial solitons are already formed in the lower modes. Therefore, when the recording light is switched off and the probe beam reads out the refractive index pattern, the channels that were formed by the lowest modes will decrease faster than those formed by the higher modes.

5. Conclusion

In conclusion, we have obtained photovoltaic lens formation and soliton propagation in Fe-doped planar waveguides in LiNbO₃ at a wavelength of 632.8 nm. The parameters of the nonlinear lenses or solitons may be controlled by combinations of active impurities and by the excitation of a suitable guided mode in the prism-coupling scheme. The storage time of waveguiding channels formed by dark solitons in the waveguides may be varied in the range from seconds to some hours. Furthermore, using techniques such as thermal fixing these channels may be made permanent.

Acknowledgment

V Shandarov gratefully acknowledges the financial support of the Russian Foundation for Basic Research (grant 00-02-17380). Financial support of the Deutsche Forschungsgemeinschaft (grant SFB 225, D9) is gratefully acknowledged.

References

- [1] Segev M, Crosignani B, Yariv A and Fischer B 1992 *Phys. Rev. Lett.* **68** 926
- [2] Singh S R and Christodoulides D N 1995 *Opt. Commun.* **118** 569
Zozulya A A and Anderson D Z 1995 *Phys. Rev. A* **51** 1520
Stegeman G I and Segev M 1999 *Science* **286** 1518
- [3] Valley G C, Segev M, Crosignani B, Yariv A, Fejer M M and Bashaw M C 1994 *Phys. Rev. A* **50** R4457
Christodoulides D N and Carvalho M I 1995 *J. Opt. Soc. Am. B* **12** 1628
- [4] Taya M, Bashaw M C, Fejer M M, Segev M and Valley G C 1995 *Phys. Rev. A* **52** 3095
- [5] Anastassiou C, Shih M F, Mitchell M, Chen Z and Segev M 1998 *Opt. Lett.* **23** 924
She W L, Lee K K and Lee W K 1999 *Phys. Rev. Lett.* **83** 3182
- [6] Kip D 1998 *Appl. Phys. B* **67** 131
- [7] Chen Z, Mitchell M, Segev M, Coskun T H and Christodoulides D N 1998 *Science* **280** 889
Chen Z, Segev M, Coskun T H, Christodoulides D N, Kivshar Y S and Afanasjev V V 1996 *Opt. Lett.* **21** 1821
- [8] Kip D and Krätzig E 1992 *Opt. Lett.* **17** 1563